



HAL
open science

Lyapunov-based robust control design for a class of switching non-linear systems subject to input saturation: application to engine control

Anhtu Nguyen, Michel Dambrine, Jimmy Lauber

► To cite this version:

Anhtu Nguyen, Michel Dambrine, Jimmy Lauber. Lyapunov-based robust control design for a class of switching non-linear systems subject to input saturation: application to engine control. *IET Control Theory & Applications*, 2014, 8 (17), pp.1789-1802. 10.1049/iet-cta.2014.0398 . hal-04307251

HAL Id: hal-04307251

<https://uphf.hal.science/hal-04307251>

Submitted on 25 Nov 2023

HAL is a multi-disciplinary open access archive for the deposit and dissemination of scientific research documents, whether they are published or not. The documents may come from teaching and research institutions in France or abroad, or from public or private research centers.

L'archive ouverte pluridisciplinaire **HAL**, est destinée au dépôt et à la diffusion de documents scientifiques de niveau recherche, publiés ou non, émanant des établissements d'enseignement et de recherche français ou étrangers, des laboratoires publics ou privés.

See discussions, stats, and author profiles for this publication at: <https://www.researchgate.net/publication/283294789>

Lyapunov-Based Robust Control Design for a Class of Switching Nonlinear Systems Subject to Input Saturation: Application to Engine Control

Article in IET Control Theory and Applications · November 2014

DOI: 10.1049/iet-cta.2014.0398

CITATIONS

41

READS

336

3 authors:



Anh-Tu Nguyen

Université Polytechnique Hauts-de-France

140 PUBLICATIONS 2,084 CITATIONS

[SEE PROFILE](#)



Michel Dambrine

Université Polytechnique Hauts-de-France

151 PUBLICATIONS 4,316 CITATIONS

[SEE PROFILE](#)



Jimmy Lauber

Université Polytechnique Hauts-de-France

154 PUBLICATIONS 2,026 CITATIONS

[SEE PROFILE](#)



Lyapunov-based robust control design for a class of switching non-linear systems subject to input saturation: application to engine control

AnhTu Nguyen, Michel Dambrine, Jimmy Lauber

LAMIH laboratory UMR CNRS 8201, University of Valenciennes, 59313 Valenciennes Cedex, France
 E-mail: nguyen.trananhthu@gmail.com

Abstract: Control technique based on the well-known Takagi–Sugeno (T–S) models offers a powerful and systematic tool to cope with complex non-linear systems. This study presents a new method to design robust H_∞ controllers stabilising the switching uncertain and disturbed T–S systems subject to control input saturation. To this end, the input saturation is taken into account in the control design under its polytopic form. The Lyapunov stability theory is used to derive the design conditions, which are formulated as a linear matrix inequality (LMI) optimisation problem. The controller design amounts to solving a set of LMI conditions with some numerical tools. In comparison with previous results, the proposed method not only provides a simple and efficient design procedure to deal with a large class of input saturated non-linear systems but also leads to less conservative design conditions. Moreover, with a simple shape criterion, the proposed approach maximises also the estimated domain of attraction included inside the validity domain of the system. The validity of the proposed method is illustrated through academic as well as real industrial examples.

1 Introduction

1.1 Motivations and related works

Over the past two decades, control technique based on the so-called Takagi–Sugeno (T–S) models [1] has become an active research topic [2]. In particular, this technique has received more and more significant attention [2, 3], since it has been successfully applied to numerous engineering applications [2, 4, 5]. The T–S models are inspired from the historical approach of fuzzy logic [6], they can be interpreted as a collection of local linear models interconnected by scalar membership functions. Then, based on a T–S representation, a model-based control will be designed to guarantee the stability and achieve some performance requirements for non-linear systems. Thanks to its polytopic structure, the main interest of T–S control approach is to make possible the extension of some linear concepts to the case of non-linear systems [2]. This control technique provides a general and systematic framework to cope with complex non-linear systems. Nevertheless, it is not always possible from a theoretical or practical point of view to use the classical T–S approach for some specific cases such as systems with singularity points [7] or systems with a too large number of sub-systems [8] (this number increases exponentially with the number of non-linearities of the original non-linear system when using the sector non-linear approach). Based on these remarks, a new switching T–S approach which allows overcoming the above drawbacks has been proposed in [7]. In this paper, we focus on this class

of switching T–S models. Indeed, a switching T–S model is composed by local T–S models and switches between them according to scheduling variables depending or not on system states. Its structure has two levels: a regional level and a local one with the associated T–S model. In Fig. 1 is illustrated the concept of switching T–S control approach, the supervisor decides which controller has to be connected in the closed loop according to the actual operating region of the non-linear system. It is worth noting that it inherits some essential features of hybrid systems [9] and retains all the information and knowledge representation capacity of T–S systems.

Among all non-linear phenomena, actuator saturation is unavoidable in almost real applications. It can severely degrade closed-loop system performance and in some cases may lead to the system instability. Motivated by this practical control aspect, a great deal of effort has been recently focused on saturated systems, see, for example, [10–12] and the references therein. In general, there are two main approaches to deal with the input saturation problem. The first one considers implicitly the saturation effect. In this approach, called ‘anti-windup’ [13], the control input is first computed by ignoring actuator saturation. Once the controller has been designed, an additional anti-windup compensator is included to handle the saturation constraints. In the second approach, the saturation effect in control design process is taken directly into account. For this, two principal synthesis techniques are considered: ‘saturated control law’ and ‘unsaturated control law’. In the latter one, the initial state domain and the design are such that the control

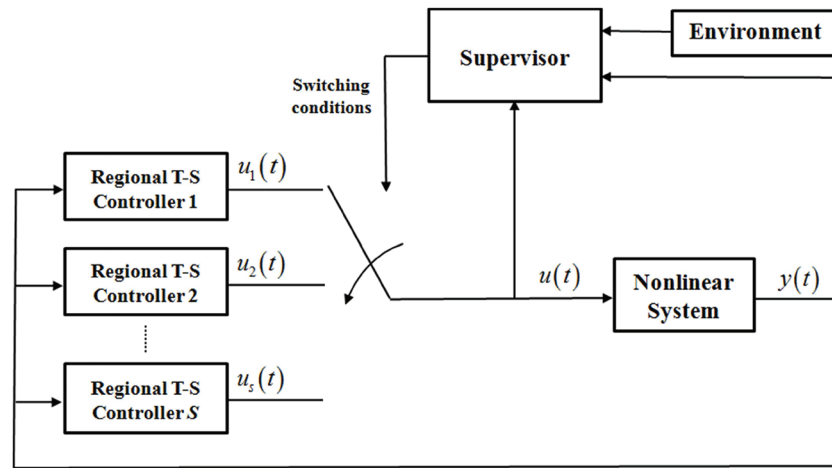


Fig. 1 Concept of switching T–S control approach

law will never reach saturation limits. Presented for instance in [2], this type of low-gain controller is very conservative and often leads to poor system performance [10, 12]. As its name indicates, the saturated control law [10] allows the saturation of the input signal which results in a better control performance. That is why this type of control laws will be addressed in this paper. It is also worth remarking that the system states are also usually bounded in engineering applications. Specifically, the validity domain of T–S models obtained with the sector non-linearity approach can be described by state constraints. Therefore the state constraints need also to be considered in control design.

1.2 Original contributions

The main focus of this paper is to propose a new ‘saturated control method’ for a class of switching uncertain and disturbed T–S models subject to control input saturation and state constraints. To that end, saturation non-linearity is directly taken into account in the design control by using its polytopic representation. Compared with the existing results, the proposed method provides more relaxed design conditions while considering many closed-loop requirements. Moreover, the estimated domain of attraction of the system is maximised which is also necessary for such a regional stability approach.

The control scheme is based on the parallel distributed compensation (PDC) concept [2] and the consideration of H_∞ performance which guarantees the γ -disturbance attenuation. By using Lyapunov stability theory, the design conditions are derived. The key point of the proposed method is to achieve conditions in linear matrix inequality (LMI) form. Thus, the controller gains can be efficiently computed with some available numerical tools [14]. Up to now, many studies have investigated the robust stabilisation of uncertain and disturbed T–S systems, see, for example, [3, 15, 16] and references therein. However, very-few results deal with the switching uncertain and disturbed T–S models subject to control input and state constraints. Our approach can be applied for a large class of switching non-linear systems.

The validity of the proposed approach is illustrated with two examples. The first academic example aims at demonstrating its great improvements compared to previous results in [7]. The second example concerning the control of a turbocharged air system of a SI engine points out clearly the usefulness of our approach in an industrial context. In

fact, the control issue of turbocharged SI engine is very challenging because of the important number of involved non-linearities. Hence, the topic is currently subject to an extensive investigation in automotive industry, see [4, 5] and references therein for more details. Using classical T–S models leads to an excessive number of sub-systems which makes difficult to design and implement the T–S controller. Another specific point for this application is that it is not possible to consider the ‘fuel-optimal strategy’ [17] to minimise the engine pumping losses with classical T–S control approach. To avoid these drawbacks, a switching T–S modelling approach for this complex non-linear system has been proposed in our previous works [4, 5, 18]. In this paper, both control input and state constraints are explicitly considered in the design procedure which was not be done in the previous results. In addition, the obtained controller, having only two tuning parameters, is easily implementable and achieves very-satisfying results. To the best of our knowledge, this is the first non-linear model-based control approach for which stability of the whole turbocharged air system can be proved while taking into account the control input constraint and the fuel-optimal strategy. Finally, this generic approach can be also generalised for other more complex turbocharging systems with several air actuators.

1.3 Organisation

The paper is organised as follows. In Section 2, the stabilisation problem of a switching uncertain T–S system subject to control input and state constraints is first introduced and some useful preliminary results needed for the control design are then presented. Section 3 is devoted to the main results of the paper and the stability of the closed-loop system is also proved based on Lyapunov theory. Section 4 provides a constructive comparison between the proposed approach and previous results via an academic example and shows also how to apply this new result to control the turbocharged air system of a SI engine. Finally, a conclusion is given in Section 5.

Notation: For an integer number r , Ω_r denotes the set $\{1, 2, \dots, r\}$. $\mathbb{R}^+ = [0, \infty)$ denotes the set of non-negative real numbers. $x_{(i)}$ is the i th element of vector x . $X_{(i)}$ and $X_{(i,j)}$ denote, respectively, the i th row and the element of i th row and j th column of matrix X . (*) stands for symmetric matrix blocks and $\text{sym}(X) = X + X^T$. $X > 0$ is used to

denote a symmetric, positive-definite matrix. I denotes the identity matrix of appropriate dimensions. For $P > 0$, denote $\mathcal{E}(P, \rho) \triangleq \{x : x^T P x \leq \rho\}$ and for brevity $\mathcal{E}(P) \equiv \mathcal{E}(P, 1)$. The real functions $\eta_1(\theta), \dots, \eta_r(\theta)$ defined on a set D are said to verify the convex sum property if $\forall i \in \Omega_r, \eta_i(\theta) \geq 0$ and $\sum_{i=1}^r \eta_i(\theta) = 1, \forall \theta \in D$. The superscript k in scalars or matrices will be used to indicate the k th operating region of the switching system. The following notations will be used, with $(k, i, j) \in \Omega_s \times \Omega_r \times \Omega_r$,

$$\begin{aligned} X_\sigma &= \sum_{k=1}^s \mu^k X^k; & Y_{\sigma\theta} &= \sum_{k=1}^s \sum_{i=1}^r \mu^k \eta_i^k Y_i^k; \\ Z_{\sigma\theta\theta} &= \sum_{k=1}^s \sum_{i=1}^r \sum_{j=1}^r \mu^k \eta_i^k \eta_j^k Z_{ij}^k \end{aligned} \quad (1)$$

where X^k, Y_i^k, Z_{ij}^k are matrices of appropriate dimensions, and the scalar functions μ^k, η_i^k satisfy the convex sum property. Note that explicit time-dependence of the variables will be often omitted when no ambiguity occurs.

2 Problem position and preliminaries results

2.1 Switching T-S system description

Consider the following uncertain non-linear switched system

$$\begin{cases} \dot{x} = (f_\sigma(\theta) + \Delta f_\sigma(\theta))x + (g_\sigma(\theta) + \Delta g_\sigma(\theta))u \\ z = (k_\sigma(\theta) + \Delta k_\sigma(\theta))x + (h_\sigma(\theta) + \Delta h_\sigma(\theta))u \end{cases} \quad (2)$$

where $x \in \mathbb{R}^{n_x}, u \in \mathbb{R}^{n_u}$ and $w \in \mathbb{R}^{n_w}$ are, respectively, the state, the control input and the disturbance vectors. The controlled output vector $z \in \mathbb{R}^{n_z}$ is used for performance purposes. The scheduling variable vector $\theta \in \mathbb{R}^{n_\theta}$ is assumed to be known and it may be functions of all signals of interest (states, measurements, external disturbances and/or time) with the exception of the control input value u . The switching signal σ takes value in Ω_s and may depend on the components of the scheduling variable vector, so that we can write with a slight abuse of notation $\sigma = \sigma(\theta)$.

It is assumed that the matrix-valued functions $f_\sigma, \Delta f_\sigma, g_\sigma, \Delta g_\sigma, k_\sigma, \Delta k_\sigma, h_\sigma$ and Δh_σ in (2) are sufficiently smooth and bounded on a given compact set \mathcal{P}_θ . For $\theta \in \mathcal{P}_\theta$, using the sector non-linearity approach [2], the system (2) can be exactly represented by a switched T-S model of the form

$$\begin{cases} \dot{x} = \sum_{k=1}^s \sum_{i=1}^r \mu^k(\theta) \eta_i^k(\theta) [\mathbb{A}_i^k x + \mathbb{B}_{w,i}^k w + \mathbb{B}_{u,i}^k u] \\ z = \sum_{k=1}^s \sum_{i=1}^r \mu^k(\theta) \eta_i^k(\theta) [\mathbb{C}_{z,i}^k x + \mathbb{D}_{w,i}^k w + \mathbb{D}_{u,i}^k u] \end{cases} \quad (3)$$

where

$$\begin{aligned} \mathbb{A}_i^k &= A_i^k + \Delta A_i^k; & \mathbb{B}_{w,i}^k &= B_{w,i}^k + \Delta B_{w,i}^k; & \mathbb{B}_{u,i}^k &= B_{u,i}^k + \Delta B_{u,i}^k \\ \mathbb{C}_{z,i}^k &= C_{z,i}^k + \Delta C_{z,i}^k; & \mathbb{D}_{w,i}^k &= D_{w,i}^k + \Delta D_{w,i}^k; & \mathbb{D}_{u,i}^k &= D_{u,i}^k + \Delta D_{u,i}^k \end{aligned} \quad (4)$$

The membership functions $\eta_i^k(\theta)$ verify the convex sum property and the indicator functions $\mu^k(\theta)$ for $k \in \Omega_s$ are

defined by

$$\mu^k(\theta) = \begin{cases} 1 & \text{if } \theta \in \mathfrak{R}_k \\ 0 & \text{otherwise} \end{cases} \quad (5)$$

where the polyhedral regions $\mathfrak{R}_k \subseteq \mathbb{R}^{n_\theta}$ constitute a non-overlapping partition of \mathcal{P}_θ . The constant matrices of appropriate dimensions $A_i^k, B_{w,i}^k, B_{u,i}^k, C_{z,i}^k, D_{w,i}^k$ and $D_{u,i}^k$ describe the nominal system which correspond to the matrix-valued functions $f_\sigma, g_\sigma, k_\sigma$ and h_σ ; and the time-varying matrices $\Delta A_i^k, \Delta B_{w,i}^k, \Delta B_{u,i}^k, \Delta C_{z,i}^k, \Delta D_{w,i}^k$ and $\Delta D_{u,i}^k$ represent the system uncertainty corresponding to the uncertain terms $\Delta f_\sigma, \Delta g_\sigma, \Delta k_\sigma$ and Δh_σ . These matrices are assumed to be bounded

$$\begin{bmatrix} \Delta A_i^k & \Delta B_{w,i}^k & \Delta B_{u,i}^k \\ \Delta C_{z,i}^k & \Delta D_{w,i}^k & \Delta D_{u,i}^k \end{bmatrix} = \begin{bmatrix} F_x^k \Theta_x [E_{A,i}^k & E_{Bw,i}^k & E_{Bu,i}^k] \\ F_z^k \Theta_z [E_{Cz,i}^k & E_{Dw,i}^k & E_{Du,i}^k] \end{bmatrix} \quad (6)$$

where $F_x^k, F_z^k, E_{A,i}^k, E_{Bw,i}^k, E_{Bu,i}^k, E_{Cz,i}^k, E_{Dw,i}^k, E_{Du,i}^k, (k, i) \in \Omega_s \times \Omega_r$ are known constant matrices of appropriate dimensions characterising the uncertainty structure and the time-varying matrices Θ_x, Θ_z with unknown, measurable elements satisfy

$$\Theta_x^T \Theta_x \leq I; \quad \Theta_z^T \Theta_z \leq I \quad (7)$$

The following assumptions are considered in this paper

Assumption 1: It is assumed that the scheduling vector θ depends only on the system state x .

Assumption 2: The control input u is subject to actuator saturation

$$\text{sat}(u_{(l)}) = \text{sign}(u_{(l)}) \min\{u_{\max(l)}, |u_{(l)}|\}; \quad \forall l \in \Omega_{nu} \quad (8)$$

where $u_{\max} \in \mathbb{R}_+^{n_u}$ denotes the saturation level vector. Note that, for sake of simplicity, the above saturation constraints are symmetric. In case of asymmetric ones—that is, when the input signals satisfy inequalities of the form $u_{\min(l)} \leq u_{(l)} \leq u_{\max(l)}$ with $u_{\min(l)} \neq -u_{\max(l)}$ —symmetry can be restored by removing and then adding a constant input $C = (u_{\min(l)} + u_{\max(l)})/2$ in the upstream and downstream of the saturation.

2.2 Control problem formulation

This paper proposes a systematic method to design a switching state feedback controller for the constrained system (3) such that the closed-loop system satisfies the following properties

(P.1) *State constraints:* For any admissible initial state, the states of the closed-loop system (3) are required to remain in the validity domain \mathcal{P}_x described by linear inequalities, with $h_m \in \mathbb{R}^{n_x}$

$$\mathcal{P}_x = \{x \in \mathbb{R}^{n_x} : h_m^T x \leq 1; \quad \forall m \in \Omega_g\} \quad (9)$$

(P.2) *Regional quadratic α -stability:* For $w = 0$, there exists a positive real number α and a quadratic function $V(x) = x^T P x$, with $P > 0$, such that $\dot{V}(x) < -2\alpha V(x)$ along the closed-loop system trajectories for any initial state in the ellipsoid $\mathcal{E}(P)$.

(P.2) *\mathcal{L}_2 -gain performance:* For a given $\gamma > 0$, there exists positive real numbers δ, ρ such that, for

any energy-bounded disturbance $w \in \mathcal{W}_\delta = \{w : \mathbb{R}^+ \rightarrow \mathbb{R}^{mv}; \int_0^\infty w^T w dt \leq \delta^{-1}\}$ and for all initial states in $\mathcal{E}(P, \rho)$, the trajectories of the closed-loop system remains in the ellipsoid $\mathcal{E}(P) \supset \mathcal{E}(P, \rho)$. Furthermore, the \mathcal{L}_2 -norm of the output signal z is bounded as follows

$$\int_0^\infty z^T z dt \leq \gamma^2 \int_0^\infty w^T w dt + \rho \quad (10)$$

2.3 Switching T-S control design

2.3.1 Polytopic model for the saturation non-linearity: In this paper, the polytopic representation proposed in [10] will be used in order to model the saturation effect. For that, let $\Gamma = \{\Gamma_p^+\}_{p \in \Omega_{2^m}}$ be the set of $(m \times m)$ diagonal matrices whose diagonal elements take the value 0 or 1, each element of Γ being indexed by an integer number in Ω_{2^m} . For any $p \in \Omega_{2^m}$, Γ_p^- denotes the element of Γ associated with Γ_p^+ such that

$$\Gamma_p^- = I - \Gamma_p^+ \quad (11)$$

Lemma 1 [10]: Let $u, v \in \mathbb{R}^m$. Suppose that $-u_{\max} < v < u_{\max}$, it follows that

$$\text{sat}(u) \in \text{co}\{\Gamma_p^+ u + \Gamma_p^- v; \quad \forall p \in \Omega_{2^m}\} \quad (12)$$

Consequently, $\text{sat}(u)$ can be represented as

$$\text{sat}(u) = \sum_{p=1}^{2^m} \xi_p (\Gamma_p^+ u + \Gamma_p^- v) \quad (13)$$

where the numbers ξ_p verify the convex sum property.

2.3.2 State feedback control law: The switching state feedback controller of the system (3) is naturally extended from the PDC concept [2] and represented as

$$u = \sum_{k=1}^s \sum_{j=1}^r \mu_k(\theta) \eta_j^k(\theta) L_j^k x \quad (14)$$

Note that the switching PDC law (14) shares the same indicator and membership functions as the switching T-S model (3). Let $\tilde{H} = \{H_j^k\}_{j \in \Omega_r, k \in \Omega_s}$ be a finite family of $(m \times n)$ matrices, the polyhedral set $\Xi(\tilde{H}, u_{\max})$ is defined by

$$\Xi(\tilde{H}, u_{\max}) = \bigcap_{k=1}^s \bigcap_{j=1}^r \Xi(H_j^k, u_{\max}) \quad (15)$$

where $\Xi(H_j^k, u_{\max})$ denotes the polyhedron

$$\Xi(H_j^k, u_{\max}) = \{x \in \mathbb{R}^{nx} : -u_{\max} < H_j^k x < u_{\max}\} \quad (16)$$

By Lemma 1, it is simple to prove that, for any $x \in \Xi(\tilde{H}, u_{\max})$, the input saturation can be expressed as

$$\text{sat}(u) = \sum_{k=1}^s \sum_{j=1}^r \sum_{p=1}^{2^m} \mu_k(\theta) \eta_j^k(\theta) \xi_p (\Gamma_p^+ L_j^k + \Gamma_p^- H_j^k) x \quad (17)$$

By substituting (17) into (3) and using the notations (1), the closed-loop system can then be rewritten as follows

$$\begin{cases} \dot{x} = [A_{\sigma\theta} + B_{u,\sigma\theta}(\Gamma_\xi^+ L_{\sigma\theta} + \Gamma_\xi^- H_{\sigma\theta})]x + B_{w,\sigma\theta} w \\ z = [C_{z,\sigma\theta} + D_{u,\sigma\theta}(\Gamma_\xi^+ L_{\sigma\theta} + \Gamma_\xi^- H_{\sigma\theta})]x + D_{w,\sigma\theta} w \end{cases} \quad (18)$$

where $\Gamma_\xi^+ = \sum_{p=1}^{2^m} \xi_p \Gamma_p^+$ and $\Gamma_\xi^- = \sum_{p=1}^{2^m} \xi_p \Gamma_p^-$.

Remark 1: In (18), the property that $\mu^k(\theta)\mu^l(\theta) = 0$ if $k \neq l$ has been used.

2.4 Maximisation of the estimate domain of attraction

Concerning the undisturbed, closed-loop system, an estimate of the attraction domain of its equilibrium point $x = 0$ will be given in the ellipsoid form $\mathcal{E}(P)$, with $P > 0$, that will be positively invariant. Since regional stability approach is adopted here, it is worth maximising the size of the ellipsoid. To this end, the idea of shape reference set proposed in [19] will be used. Let $X_R \subset \mathbb{R}^{nx}$ be a prescribed bounded convex set containing the origin. Finding the largest ellipsoid $\mathcal{E}(P)$ can be formulated as the following optimisation problem

$$\max_{\tau, P > 0} \tau \text{ subject to : } \tau X_R \subset \mathcal{E}(P) \quad (19)$$

There are two typical choices for reference set X_R . The first one is an ‘ellipsoid’ defined as

$$X_R = \{x \in \mathbb{R}^{nx} : x^T R x \leq 1\} \quad (20)$$

where $R > 0$. The second one is a ‘polyhedron’ defined as

$$X_R = \text{co}\{x_{01}, x_{02}, \dots, x_{0l}\} \quad (21)$$

where $x_{01}, x_{02}, \dots, x_{0l}$ are a priori given points in \mathbb{R}^{nx} .

For these two choices of set X_R , optimisation problem (19) can be rewritten as

- If the reference shape X_R is given by the ellipsoid (20), then $\tau X_R \subset \mathcal{E}(P)$ is equivalent to the condition

$$\frac{R}{\tau^2} \geq P \quad (22)$$

Let $\lambda = 1/\tau^2$ and $Q = P^{-1}$, and using Schur complement lemma, the problem (19) can be expressed as the LMI optimisation problem of finding the minimum value of λ satisfying the inequality

$$\begin{bmatrix} \lambda R & I \\ I & Q \end{bmatrix} \geq 0 \quad (23)$$

- If X_R is the polyhedron (21), then $\tau X_R \subset \mathcal{E}(P)$ is equivalent to

$$\tau^2 (x_{0i})^T (P) x_{0i} \leq 1; \quad \forall i \in \Omega_l \quad (24)$$

This inequality can also be reformulated in LMI form as

$$\begin{bmatrix} \lambda & * \\ x_{0i} & Q \end{bmatrix} \geq 0; \quad \forall i \in \Omega_l \quad (25)$$

2.5 Other preliminary results

Some other results that will be useful in the proof of our main result are recalled below.

Lemma 2 [10]: The ellipsoid set $\mathcal{E}(P)$ is contained in the polyhedral set $\Xi(H, u_{\max})$ if and only if

$$(H_{(l)})(P^{-1})(H_{(l)})^T \leq u_{\max(l)}^2, \quad \forall l \in \Omega_{nu} \quad (26)$$

where $H_{(l)}$ is the l th row of the matrix H .

Lemma 3 [19]: The ellipsoid $\mathcal{E}(P)$ is included in the polyhedral set \mathcal{P}_x defined in (9) if and only if

$$\begin{bmatrix} P & h_m \\ * & 1 \end{bmatrix} \geq 0; \quad \forall m \in \Omega_q \quad (27)$$

Lemma 4 [20]: Let X, Y and Δ be real matrices of appropriate dimensions and $\Delta^T \Delta \leq I$. Then, for any scalar $\varepsilon > 0$, the following inequality holds

$$X \Delta Y + Y^T \Delta^T X^T \leq \varepsilon X X^T + \varepsilon^{-1} Y^T Y \quad (28)$$

Lemma 5 [21]: Let $\Upsilon_{ij}, (i, j) \in \Omega_r \times \Omega_r$ be symmetric matrices of appropriate dimensions and η_1, \dots, η_r be a family of numbers satisfying the convex sum property. If

$$\begin{cases} \Upsilon_{ii} < 0; & \forall i \in \Omega_r \\ \frac{2}{r-1} \Upsilon_{ii} + \Upsilon_{ij} + \Upsilon_{ji} < 0; & \forall (i, j) \in \Omega_r \times \Omega_r \text{ and } i \neq j \end{cases} \quad (29)$$

Then

$$\sum_{i=1}^r \sum_{j=1}^r \eta_i \eta_j \Upsilon_{ij} < 0 \quad (30)$$

Note that more performing relaxation results exist such as in [22, 23]. However, Lemma 5 constitutes a good trade-off between complexity and conservatism since it does not require the introduction of auxiliary variables.

3 Main results

This section provides the LMI-based solution for the control design problem stated in Section 2.2.

Theorem 1: Given positive real numbers α, γ and a set X_R defined as in (20) (or (21)), if there exists matrices $Q > 0, Y_j^k, Z_j^k$, and positive real numbers $\lambda, \delta, \rho, \varepsilon_{x,ij}, \varepsilon_{z,ij}$ (for $(k, i, j) \in \Omega_s \times \Omega_r \times \Omega_r$), such that (23) (or (25)) holds

and satisfying also the following inequalities

$$\begin{bmatrix} Q & \\ Z_{j(l)}^k & u_{\max(l)}^* \end{bmatrix} \geq 0; \quad \forall (k, l, j) \in \Omega_s \times \Omega_{nu} \times \Omega_r \quad (31)$$

$$\begin{bmatrix} Q & Q h_m \\ * & 1 \end{bmatrix} \geq 0; \quad \forall m \in \Omega_q \quad (32)$$

$$\Upsilon_{iip}^k < 0; \quad \forall (k, i, p) \in \Omega_s \times \Omega_r \times \Omega_{2m} \quad (33)$$

$$\frac{2}{r-1} \Upsilon_{iip}^k + \Upsilon_{ijp}^k + \Upsilon_{jip}^k < 0; \quad \forall (k, i, j, p) \in \Omega_s \times \Omega_r \times \Omega_r \times \Omega_{2m}, \quad i \neq j \quad (34)$$

$$\begin{bmatrix} 1 - \rho & \gamma \\ \gamma & \delta \end{bmatrix} \geq 0 \quad (35)$$

where $Z_{j(l)}^k$ denotes the l th row of matrix Z_j^k and Υ_{ijp}^k is defined in (37). Then, the switching state feedback controller (14) with

$$L_j^k = Y_j^k Q^{-1}; \quad \forall (k, j) \in \Omega_s \times \Omega_r \quad (36)$$

solves the control problem stated in Section 2.2. (see (37))

Proof: Considering the Lyapunov function $V(x) = x^T P x$. Let us define $Q \triangleq P^{-1}$ and $Z_j^k \triangleq H_j^k Q$, using the Schur complement lemma on (31), it follows that

$$(Z_{j(l)}^k)(Q^{-1})(Z_{j(l)}^k)^T \leq u_{\max}(l)^2; \quad \forall (l, j, k) \in \Omega_{nu} \times \Omega_r \times \Omega_s \quad (38)$$

which, by Lemma 2, is equivalent to $\mathcal{E}(P) \subset \Xi(\tilde{H}, u_{\max})$. \square

Pre- and post-multiplying the condition (27) with $\text{diag}(Q, 1)$, this condition is then found to be equivalent to (32). This fact, by Lemma 3, means that $\mathcal{E}(P) \subset \mathcal{P}_x$. This fact proves *Property (P.1)* stated in Section 2.2.

To continue, let us introduce the following notations for brevity (see (39))

$$\Upsilon_{ijp}^k \triangleq \begin{bmatrix} \text{sym}(A_i^k Q + B_{u,i}^k (\Gamma_p^+ Y_j^k + \Gamma_p^- Z_j^k) + \alpha Q) & * & * & * & * & * & * \\ (B_{w,i}^k)^T & -\gamma^2 I & * & * & * & * & * \\ C_{z,i}^k Q + D_{u,i}^k (\Gamma_p^+ Y_j^k + \Gamma_p^- Z_j^k) & D_{w,i}^k & -I & * & * & * & * \\ \varepsilon_{x,ij}^k (F_x^k)^T & 0 & 0 & -\varepsilon_{x,ij}^k I & * & * & * \\ E_{A,i}^k Q + E_{Bu,i}^k (\Gamma_p^+ Y_j^k + \Gamma_p^- Z_j^k) & E_{Bw,i}^k & 0 & 0 & -\varepsilon_{x,ij}^k I & * & * \\ 0 & 0 & \varepsilon_{z,ij}^k (F_z^k)^T & 0 & 0 & -\varepsilon_{z,ij}^k I & * \\ E_{Cz,i}^k Q + E_{Du,i}^k (\Gamma_p^+ Y_j^k + \Gamma_p^- Z_j^k) & E_{Dw,i}^k & 0 & 0 & 0 & 0 & -\varepsilon_{z,ij}^k I \end{bmatrix} \quad (37)$$

$$\begin{aligned} Y_j^k &\triangleq L_j^k Q; & S_{\sigma\xi\theta} &\triangleq E_{A,\sigma\theta} + E_{Bu,\sigma\theta} (\Gamma_\xi^+ L_{\sigma\theta} + \Gamma_\xi^- H_{\sigma\theta}); & T_{\sigma\xi\theta} &\triangleq E_{Cz,\sigma\theta} + E_{Du,\sigma\theta} (\Gamma_\xi^+ L_{\sigma\theta} + \Gamma_\xi^- H_{\sigma\theta}) \\ U_{\sigma\xi\theta} &\triangleq (A_{\sigma\theta} + B_{u,\sigma\theta} (\Gamma_\xi^+ L_{\sigma\theta} + \Gamma_\xi^- H_{\sigma\theta}))^T P + \alpha P; & \mathbb{U}_{\sigma\xi\theta} &\triangleq (\mathbb{A}_{\sigma\theta} + \mathbb{B}_{u,\sigma\theta} (\Gamma_\xi^+ L_{\sigma\theta} + \Gamma_\xi^- H_{\sigma\theta}))^T P + \alpha P \\ V_{\sigma\xi\theta} &\triangleq C_{z,\sigma\theta} + D_{u,\sigma\theta} (\Gamma_\xi^+ L_{\sigma\theta} + \Gamma_\xi^- H_{\sigma\theta}); & \mathbb{V}_{\sigma\xi\theta} &\triangleq \mathbb{C}_{z,\sigma\theta} + \mathbb{D}_{u,\sigma\theta} (\Gamma_\xi^+ L_{\sigma\theta} + \Gamma_\xi^- H_{\sigma\theta}) \end{aligned} \quad (39)$$

Assuming $x \in \Xi(\tilde{H}, u_{\max}) \cap \mathcal{P}_x$, the following expression is obtained from (18)

$$\Lambda \triangleq \dot{V}(x) + 2\alpha V(x) + z^T z - \gamma^2 w^T w = \begin{bmatrix} x \\ w \end{bmatrix}^T \Phi \begin{bmatrix} x \\ w \end{bmatrix} \quad (40)$$

where

$$\Phi \triangleq \begin{bmatrix} \text{sym}(U_{\sigma\xi\theta}) & * \\ \mathbb{B}_{w,\sigma\theta}^T P & -\gamma^2 I \end{bmatrix} + \begin{bmatrix} \mathbb{V}_{\sigma\xi\theta}^T \\ \mathbb{D}_{w,\sigma\theta}^T \end{bmatrix} \begin{bmatrix} \mathbb{V}_{\sigma\xi\theta}^T \\ \mathbb{D}_{w,\sigma\theta}^T \end{bmatrix}^T \quad (41)$$

Then applying the Schur complement lemma for (41), the condition $\Lambda < 0$ holds if and only if

$$\Psi \triangleq \begin{bmatrix} \text{sym}(U_{\sigma\xi\theta}) & * & * \\ \mathbb{B}_{w,\sigma\theta}^T P & -\gamma^2 I & * \\ \mathbb{V}_{\sigma\xi\theta} & \mathbb{D}_{w,\sigma\theta} & -I \end{bmatrix} < 0 \quad (42)$$

From (6) and (42), Ψ can be decomposed into two parts: a ‘nominal’ part Ψ_0 and an ‘uncertain’ part $\Delta\Psi$ as $\Psi \triangleq \Psi_0 + \Delta\Psi$ where

$$\Psi_0 = \begin{bmatrix} \text{sym}(U_{\sigma\xi\theta}) & * & * \\ B_{w,\sigma\theta}^T P & -\gamma^2 I & * \\ V_{\sigma\xi\theta} & D_{w,\sigma\theta} & -I \end{bmatrix} \quad (43)$$

and

$$\Delta\Psi = \text{sym}\{[(PF_{x,\sigma})^T \ 0 \ 0]^T \Theta_x [S_{\sigma\xi\theta} \ E_{Bw,\sigma\theta} \ 0]\} + \text{sym}\{[0 \ 0 \ (F_{z,\sigma})^T]^T \Theta_z [T_{\sigma\xi\theta} \ E_{Dw,\sigma\theta} \ 0]\} \quad (44)$$

Given $\varepsilon_{x,ij}^k > 0, \varepsilon_{z,ij}^k > 0, \forall (k, i, j) \in \Omega_s \times \Omega_r \times \Omega_r$, using previous notations, Lemma 4 and again the Schur complement lemma, the inequality (42) holds if the condition (46) is verified (see (45))

Moreover, using congruence with $\text{diag}[Q, I, I, I, I, I, I]$, the condition (45) is equivalent to (47) (see (46))

Now, applying Lemma 5 with inequalities (33) and (34), the inequality (46) is proved. Hence, we have shown that,

if $x \in \Xi(\tilde{H}, u_{\max}) \cap \mathcal{P}_x$, then

$$\dot{V}(x) + 2\alpha V(x) + z^T z - \gamma^2 w^T w < 0 \quad (47)$$

• Assume $w = 0, \forall t \geq 0$, it follows from (5) that

$$\dot{V}(x) < -2\alpha V(x) \quad (48)$$

which implies that the set $\mathcal{E}(P)$ is positively invariant with respect to the closed-loop system and for $\forall x(0) \in \mathcal{E}(P)$, the trajectory will converge exponentially to the origin with a decay rate α . This fact proves *Property (P.2)* in Section 2.2.

• Assume now that $w \in \mathcal{W}_\delta$, integrating both sides of (5) from 0 to T_f , where $T_f \in \mathbb{R}^+$, it follows that

$$V(x(T_f)) < V(x(0)) + \gamma^2 \int_0^{T_f} w^T w dt - \int_0^{T_f} z^T z dt \quad (49)$$

From (35) and (49), it can be deduced that $V(x(T_f)) < \rho + \gamma^2 \delta^{-1} < 1$. Hence, it can be easily shown that, for any initial state in $\mathcal{E}(P, \rho)$, the closed-loop trajectory is confined in the set $\mathcal{E}(P) \subset \Xi(\tilde{H}, u_{\max})$. Furthermore, from (49) and considering the limit case $T_f \rightarrow \infty$, we obtain $\int_0^\infty z^T z dt \leq \gamma^2 \int_0^\infty w^T w dt + V(x(0))$, this means that the \mathcal{L}_2 -norm of the output signal z is upper bounded by $\|z\|_2^2 \leq \gamma^2 \|w\|_2^2 + \rho$. These facts prove *Property (P.3)* stated in Section 2.2.

Remark 2: When $x(0) \neq 0$, there is a trade-off between the size of the set of admissible initial conditions and the maximal energy level δ of the disturbances, that is, the lower is the admissible δ , the larger is the estimate domain of attraction $\mathcal{E}(P)$ [24].

Remark 3: Theorem 1 provides LMI conditions to solve the control problem stated in Section 2.2 without any guaranty on the size of the estimate domain of attraction. As shown in Section 2.4, maximisation of this domain amounts to maximise τ (or to minimise λ). Hence, the problem of maximising the estimate domain of attraction can be formulated as

$$\min \lambda \text{ subject to : LMI conditions in Theorem 1} \quad (50)$$

$$\begin{bmatrix} \text{sym}(U_{\sigma\xi\theta}) & * & * & * & * & * & * \\ B_{w,\sigma\theta}^T P & -\gamma^2 I & * & * & * & * & * \\ V_{\sigma\xi\theta} & D_{w,\sigma\theta} & -I & * & * & * & * \\ \varepsilon_{x,\sigma\theta\theta} F_{x,\sigma}^T P & 0 & 0 & -\varepsilon_{x,\sigma\theta\theta} I & * & * & * \\ S_{\sigma\xi\theta} & E_{Bw,\sigma\theta} & 0 & 0 & -\varepsilon_{x,\sigma\theta\theta} I & * & * \\ 0 & 0 & \varepsilon_{z,\sigma\theta\theta} F_{z,\sigma}^T & 0 & 0 & -\varepsilon_{z,\sigma\theta\theta} I & * \\ T_{\sigma\xi\theta} & E_{Dw,\sigma\theta} & 0 & 0 & 0 & 0 & -\varepsilon_{z,\sigma\theta\theta} I \end{bmatrix} < 0 \quad (45)$$

$$\begin{bmatrix} \text{sym}(A_{\sigma\theta} Q + B_{u,\sigma\theta} (\Gamma_\xi^+ Y_{\sigma\theta} + \Gamma_\xi^- Z_{\sigma\theta}) + \alpha Q) & * & * & * & * & * & * \\ B_{w,\sigma\theta}^T & -\gamma^2 I & * & * & * & * & * \\ C_{z,\sigma\theta} Q + D_{u,\sigma\theta} (\Gamma_\xi^+ Y_{\sigma\theta} + \Gamma_\xi^- Z_{\sigma\theta}) & D_{w,\sigma\theta} & -I & * & * & * & * \\ \varepsilon_{x,\sigma\theta\theta} F_{x,\sigma}^T & 0 & 0 & -\varepsilon_{x,\sigma\theta\theta} I & * & * & * \\ E_{A,\sigma\theta} Q + E_{Bu,\sigma\theta} (\Gamma_\xi^+ Y_{\sigma\theta} + \Gamma_\xi^- Z_{\sigma\theta}) & E_{Bw,\sigma\theta} & 0 & 0 & -\varepsilon_{x,\sigma\theta\theta} I & * & * \\ 0 & 0 & \varepsilon_{z,\sigma\theta\theta} F_{z,\sigma}^T & 0 & 0 & -\varepsilon_{z,\sigma\theta\theta} I & * \\ E_{Cz,\sigma\theta} Q + E_{Du,\sigma\theta} (\Gamma_\xi^+ Y_{\sigma\theta} + \Gamma_\xi^- Z_{\sigma\theta}) & E_{Dw,\sigma\theta} & 0 & 0 & 0 & 0 & -\varepsilon_{z,\sigma\theta\theta} I \end{bmatrix} < 0 \quad (46)$$

It is worth remarking that X_R defines the directions in which we want to maximise $\mathcal{E}(P)$.

4 Design examples

A. Example 1: Comparison Study

To demonstrate objectively that our approach provides less conservative design conditions and can achieve larger estimate domain of attraction than the ‘reference approach’ [7], let us consider the following system from [7] without any special closed-loop performance (decay rate, model uncertainty, L_2 -gain performance): (see equation at the bottom of the page)

For this example, the following assumptions are considered for the comparison purpose. Firstly, the state vector $x^T \triangleq [x_1, x_2]$ always remains in the validity domain $\mathcal{P}_x = \{(x_1, x_2) : |x_1| \leq 2; |x_2| \leq 2\}$. Secondly, the control saturation limit is: $u_{max} = 3$.

Fig. 2 shows the feasibility solution domains according to the system initial conditions for both approaches. The marks (*) and (□) indicate, respectively, the existence of feasible solution obtained with our approach and the reference one. It is clear that the proposed approach outperforms the previous result in term of relaxation. Note that the solution computation of our approach does not depend on the initial conditions of the system.

To compare both approaches in term of the size of the domain of attraction, let us take $x_0 = 0$ for the approach proposed in [7] and for our approach, the reference shape is chosen as $X_R = \mathcal{E}(R)$ with $R = I$. Fig. 3 shows clearly that the new result allows achieving a larger estimate domain of attraction and this domain is maximised inside the validity domain \mathcal{P}_x .

B. Example 2: Control of the air system of a turbocharged spark ignited (TCSI) engine

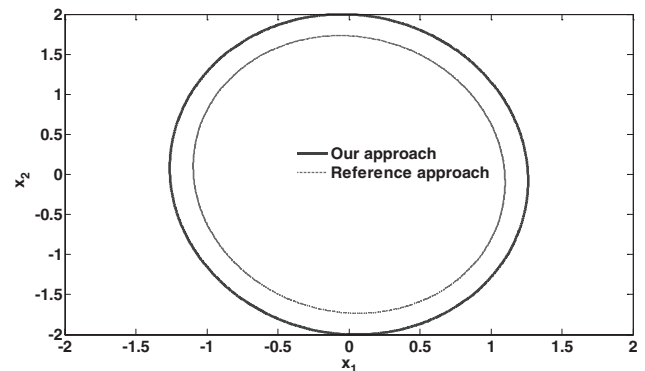


Fig. 3 Estimated domain of attraction obtained with both approaches (with $x_0 = 0$ for reference approach)

Hereafter, after a very brief description of the air system of a TCSI engine, the control approach proposed in Section 3 will be applied to control the air actuators. The model was built with the real data of a four-cylinder TCSI engine from Renault. At the end of this section, a series of trials is carried out to show the performance of the controller. The notations concerning the studied turbocharged air system are shown in Table 1.

4.1 System description and turbocharged air system control strategy

The goal here is to control a fixed geometry TCSI engine equipped with a wastegate and electronic throttle. A sketch of the considered system is depicted in Fig. 4. The ambient fresh air is boosted when passing through the compressor. This compressed air is used to burn the fuel in the cylinder where the combustion occurs, resulting in the production of the engine torque. The remaining energy (in the

Region 1: $x_2 \geq 1$

$$A_1^1 = \begin{bmatrix} 1 & -0.5 \\ -1 & 0 \end{bmatrix}; \quad A_2^1 = \begin{bmatrix} -1 & -0.5 \\ 1 & 0 \end{bmatrix};$$

$$B_{u,1}^1 = B_{u,2}^1 = \begin{bmatrix} 1 & 0 \\ 0 & 1 \end{bmatrix}$$

Region 2: $x_2 < 1$

$$A_1^2 = \begin{bmatrix} -5 & -4 \\ -1 & -2 \end{bmatrix}; \quad A_2^2 = \begin{bmatrix} -2 & -4 \\ 20 & -2 \end{bmatrix}; \quad B_{u,1}^2 = \begin{bmatrix} -0.1 & 0 \\ 0 & 0.1 \end{bmatrix};$$

$$B_{u,2}^2 = \begin{bmatrix} 0 & 0.1 \\ 1 & 0 \end{bmatrix}$$

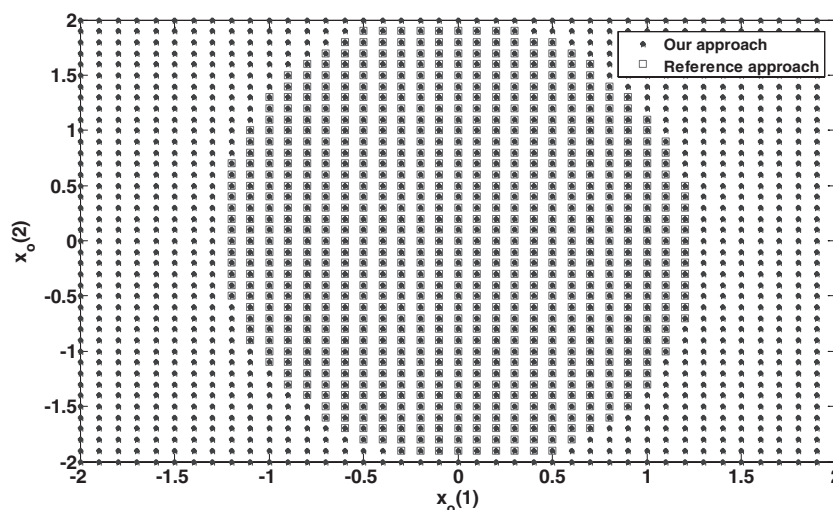


Fig. 2 Set of solutions according to the system initial conditions of our approach (●) and the reference approach (□)

Table 1 Notations of turbocharged air system of a SI engine

Symbol	Quantity	Unit	Symbol	Quantity	Unit
Π_{thr}	throttle pressure ratio	—	D_{cyl}	cylinder mass air flow	kg/s
Π_{wg}	wastegate pressure ratio	—	D_{fuel}	fuel injected flow	kg/s
Π_{comp}	compressor pressure ratio	—	V_{exh}	exhaust manifold volume	m^3
Π_{turb}	turbine pressure ratio	—	V_{man}	intake manifold volume	m^3
P_{boost}	boost pressure	Pa	V_{cyl}	cylinder volume	m^3
P_{man}	intake pressure	Pa	N_e	engine speed	rpm
P_{exh}	exhaust pressure	Pa	\dot{P}_{comp}	compressor power	W
P_{amb}	atmospheric pressure	Pa	\dot{P}_{turb}	turbine power	W
T_{amb}	atmospheric temperature	$^{\circ}K$	η_{comp}	compressor isentropic efficiency	—
T_{man}	intake manifold temperature	$^{\circ}K$	η_{turb}	turbine isentropic efficiency	—
T_{exh}	exhaust manifold temperature	$^{\circ}K$	η_{vol}	engine volumetric efficiency	—
D_{thr}	throttle mass air flow	kg/s	λ_s	stoichiometric air/fuel ratio	—
D_{wg}	wastegate mass air flow	kg/s	γ	ratio of specific heats	—
D_{comp}	compressor mass air flow	kg/s	R	ideal gas constant	J/kg $^{\circ}K$
D_{turb}	turbine mass air flow	kg/s	C_p	specific heats at constant pressure	J/kg $^{\circ}K$

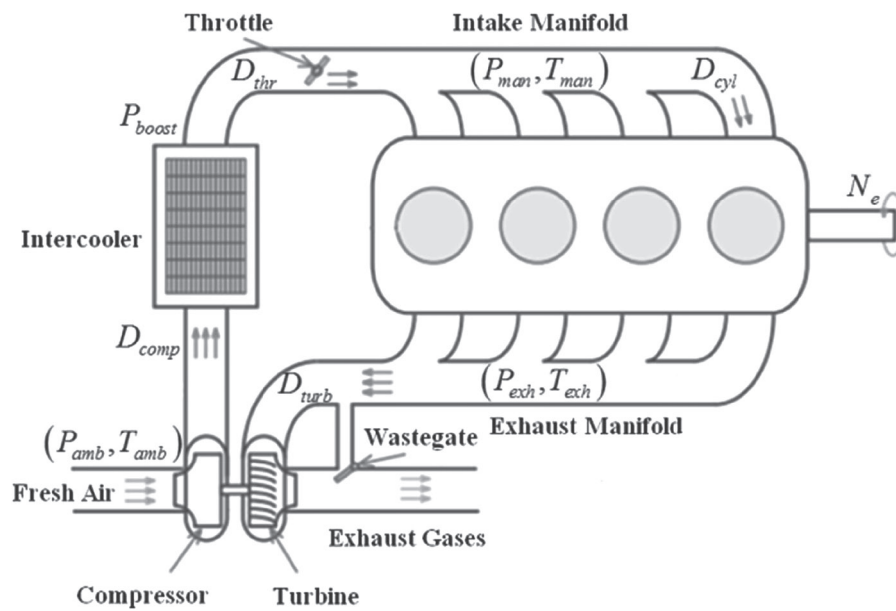


Fig. 4 Schematic representation of a TCSI engine

form of enthalpy) contained in the exhaust gases exits the system through the turbine. A part of this energy is recovered to drive the compressor via the turbocharger shaft whose dynamics are the consequences of the energy balance between the compressor and the turbine. There are two air actuators available on the studied air system:

- The throttle allows controlling directly the pressure in the intake manifold.
- The wastegate is used to control the exhaust gases flowing to the turbine by diverting a part of this flow. It allows controlling indirectly the boost pressure in the upstream of the throttle.

Conventional SI engines operate at stoichiometry which results directly in the tight connection between torque response and intake pressure P_{man} . The goal of the air system management is therefore to control this pressure. The readers can refer to our previous works [4, 5, 18] for more details concerning the state-of-the-art on turbocharged air system control issue. As highlighted in these works, to minimise

the engine pumping losses, the throttle should be fully open at high load and the boost pressure $P_{boost} \simeq P_{man}$ is controlled by the wastegate in this case. Only at low load, the throttle is activated to track the low intake pressure P_{man} . This strategy leads to the switching nature of the proposed controller.

4.2 Turbocharged air system modelling

Applicable models of a TCSI engine are well documented in [25]. In the sequel, only some key elements of the turbocharged air system and primary dependencies are recalled.

4.2.1 Intake and exhaust manifolds dynamics: The pressure dynamics in the intake and exhaust manifolds are derived from the ideal gas relationship as

$$\begin{cases} \dot{P}_{man} = \frac{RT_{man}}{V_{man}} (D_{thr} - D_{cyl}) \\ \dot{P}_{exh} = \frac{RT_{exh}}{V_{exh}} ((D_{cyl} + D_{fuel}) - (D_{turb} + D_{wg})) \end{cases} \quad (51)$$

4.2.2 Actuator valves: The mass air flows through the air actuators (throttle and wastegate) in (51) are modelled as [25]

$$D_{thr} = \Phi(\Pi_{thr}^*) \frac{P_{boost}}{\sqrt{RT_{man}}} u_{thr}; \quad D_{wg} = \Phi(\Pi_{wg}^*) \frac{P_{exh}}{\sqrt{RT_{exh}}} u_{wg} \quad (52)$$

where $\Phi(\Pi) \triangleq \sqrt{((2\gamma)/(\gamma-1))(\Pi^{2/\gamma} - \Pi^{(\gamma+1)/\gamma})}$; $\Pi_{thr}^* \triangleq \max(\Pi_{thr}, \varphi)$; $\Pi_{wg}^* \triangleq \max(\Pi_{wg}, \varphi)$ and $\varphi \triangleq (2/(\gamma+1))^{(\gamma/(\gamma-1))}$. Moreover, the physical command constraints for the air actuators are

$$S_{thr,min} \leq u_{thr} \leq S_{thr,max}; \quad S_{wg,min} \leq u_{wg} \leq S_{wg,max} \quad (53)$$

4.2.3 Turbocharger dynamics: The rotational speed of the turbocharger is modelled using Newton's second law

$$\frac{d}{dt} \left(\frac{1}{2} J_{tc} N_{tc}^2 \right) = \mathbb{P}_{turb} - \mathbb{P}_{comp} \quad (54)$$

where J_{tc} is the inertia of the turbocharger. From the first thermodynamics law, the power consumed by the compressor and the power delivered by the turbine are given

$$\begin{aligned} \mathbb{P}_{comp} &= D_{comp} C_p T_{amb} \frac{1}{\eta_{comp}} (\Pi_{comp}^{((\gamma-1)/\gamma)} - 1); \\ \mathbb{P}_{turb} &= D_{turb} C_p T_{exh} \eta_{turb} \left(1 - \Pi_{turb}^{((1-\gamma)/\gamma)} \right) \end{aligned} \quad (55)$$

where $\Pi_{comp} \triangleq P_{boost}/P_{amb}$ ($\Pi_{turb} \triangleq P_{turb}/P_{exh}$) is the compressor (turbine) pressure ratio and η_{comp} (η_{turb}) is the isentropic efficiency of the compressor (turbine). The compressor pressure ratio, the turbine mass air flow and efficiencies are mapped.

4.2.4 Turbocharged air system dynamics: From (1) and (2), and (4) and (5), the three main dynamics of the turbocharged air system can be rewritten as

$$\begin{cases} \frac{d}{dt} \left(\frac{1}{2} J_{tc} N_{tc}^2 \right) = \mathbb{P}_{turb} - \mathbb{P}_{comp} \\ \dot{P}_{man} = \frac{RT_{man}}{V_{man}} (D_{thr} - D_{cyl}) \\ \dot{P}_{exh} = \frac{RT_{exh}}{V_{exh}} ((D_{cyl} + D_{fuel}) - (D_{turb} + D_{wg})) \end{cases} \quad (56)$$

The model (56) describes accurately the three dynamics governing the turbocharged air system of an SI engine. However, this system is very complex from control point of view. Applying directly the classical T-S control technique for this system would not be an appropriate solution because of its large number of non-linearities. In our previous works [4, 5], we have showed that this turbocharged air system can be seen as a switching system with two operating regions separated according to the pressure ratio $\Pi \triangleq P_{man}/P_{amb}$. This fact has two major advantages. Firstly, it allows reducing the complexity of the final model which leads to less number of sub-systems in the final switching T-S model. Secondly, the classical T-S models are not able to deal with the strategy to minimise the engine pumping losses [17] whereas the considered switching T-S model can fully take into account this strategy. The two operating regions are defined as follows, with $\varepsilon \simeq 1.1$:

• *Region 1:* $\Pi \leq \varepsilon$ (*low load region*): The system dynamics in this region is obtained from (51) and (52)

$$\dot{P}_{man} = f_2(\cdot) u_{thr} - f_1(\cdot) P_{man} \quad (57)$$

where the non-linearities are

$$f_1(\cdot) = \frac{RT_{man}}{V_{man} P_{man}} D_{cyl}; \quad f_2(\cdot) = \frac{RT_{man}}{V_{man}} \Phi_{thr}(\Pi_{thr}) \quad (58)$$

• *Region 2:* $\Pi > \varepsilon$ (*high load region*): The reference model in Region 2 is given by [4]

$$\dot{P}_{man} = g_1(\cdot) P_{man} - g_2(\cdot) u_{wg} \quad (59)$$

where

$$\begin{aligned} g_1(\cdot) &= \frac{2}{J_{tc} A_{tc}} \left[\alpha_1 \left(1 + \frac{1}{\lambda_s} \right) - \alpha_2 \right] \alpha_3; \\ g_2(\cdot) &= \frac{2}{J_{tc} A_{tc}} \alpha_1 \Phi_{wg}(\Pi_{wg}) \end{aligned} \quad (60)$$

The parameters

$$\begin{aligned} \alpha_1 &= C_p T_{exh} \eta_{turb} \left(1 - \Pi_{turb}^{((1-\gamma)/\gamma)} \right) \\ \alpha_2 &= \frac{C_p T_{amb}}{\eta_{comp}} (\Pi_{comp}^{((\gamma-1)/\gamma)} - 1) \\ \alpha_3 &= \frac{\eta_{vol} V_{cyl} N_e}{30RT_{man}} \end{aligned}$$

depend on the engine operating conditions.

Remark 4: The successful application of the control-based model (57) for Region 1 has been experimentally achieved in [26]. The simplified model (59) for Region 2 is obtained after neglecting the fast pressures dynamics by using the singular perturbations theory which is experimentally justified in [27]. Moreover, at high load, the turbocharger square speed can be approximated by a linear function of the boost pressure $P_{boost} \simeq P_{man}$, that is, $N_{tc}^2 = A_{tc} P_{man} + B_{tc}$.

4.3 Switching robust control design

It is worth remarking that the studied system has only one state (the intake pressure) which is also the measured output and the controlled output, that is, $x = y = z = P_{man}$. Two non-linearities in each local model (57) and (59) are bounded since the system state is constrained $P_{man,min} \leq P_{man} \leq P_{man,max}$, with $P_{man,min} = 0.35$ (bar) and $P_{man,max} = 2$ (bar). Then, they can be represented as

$$\begin{cases} f_i \leq f_i(\cdot) \leq \bar{f}_i \\ g_j \leq g_j(\cdot) \leq \bar{g}_j \end{cases} \quad \text{and} \quad \begin{cases} f_i(\cdot) = \omega_{1i}^1 \bar{f}_i + \omega_{2i}^1 f_i \\ g_j(\cdot) = \omega_{1j}^2 \bar{g}_j + \omega_{2j}^2 g_j \end{cases} \quad (61)$$

where, $(i, j) \in \Omega_2 \times \Omega_2$

$$\begin{aligned} \omega_{1i}^1 &= \frac{f_i(\cdot) - \bar{f}_i}{\bar{f}_i - f_i}; & \omega_{2i}^1 &= 1 - \omega_{1i}^1; \\ \omega_{1j}^2 &= \frac{g_j(\cdot) - \bar{g}_j}{\bar{g}_j - g_j}; & \omega_{2j}^2 &= 1 - \omega_{1j}^2 \end{aligned} \quad (62)$$

Thus, the global switching system has two separated regions and the T-S model in each region has four linear models.

The normalised membership functions in each local region are given by (see (63))

For tracking control purpose, it is well known that an integral action in the control law is necessary to reject some static disturbance. This amounts adding a new state whose dynamics is defined as, with the intake pressure reference $y_{ref} \triangleq P_{man,ref}$

$$\dot{x}_{int} = y_{ref} - y \quad (64)$$

Then, the proposed controller of this application is a dynamic one which can be obtained from (14) and (64)

$$\begin{cases} \dot{x}_{int} = -x + y_{ref} \\ u = \sum_{k=1}^s \sum_{j=1}^r \mu_k(\theta) \eta_j^k(\theta) (L_j^k x + K_j^k x_{int}) \end{cases} \quad (65)$$

Let us define $\bar{x} \triangleq [P_{man}; x_{int}]$ and $u \triangleq [u_{thr}; u_{wg}]$. Then, the global closed-loop system can be represented as follows (see (66))

where the scheduling variable vector θ corresponds to the non-linearities $f_i(\cdot)$ or $g_i(\cdot)$, $i = 1, 2$ according to the considered operating region, and the matrices of the extended systems are given by, with $\tilde{w}^T = [w^T, y_{ref}]$

$$\begin{aligned} \bar{A}_i^k &= \begin{bmatrix} A_i^k & 0 \\ -C_i^k & 0 \end{bmatrix}; & \Delta \bar{A}_i^k &= \begin{bmatrix} \Delta A_i^k & 0 \\ 0 & 0 \end{bmatrix}; & \bar{C}_i^k &= [C_i^k \quad 0] \\ \bar{B}_{u,i}^k &= \begin{bmatrix} B_{u,i}^k \\ 0 \end{bmatrix}; & \Delta \bar{B}_{u,i}^k &= \begin{bmatrix} \Delta B_{u,i}^k \\ 0 \end{bmatrix}; \\ \bar{B}_{w,i}^k &= \begin{bmatrix} B_{w,i}^k \\ 1 \end{bmatrix}; & \bar{D}_i^k &= \begin{bmatrix} D_i^k \\ 0 \end{bmatrix} \end{aligned} \quad (67)$$

In this work, a maximum of 10% parametric uncertainties are considered

$$\begin{cases} |\Delta f_1(\cdot)| \leq 0.1 f_1(\cdot); & |\Delta f_2(\cdot)| \leq 0.1 f_2(\cdot) \\ |\Delta g_1(\cdot)| \leq 0.1 g_1(\cdot); & |\Delta g_2(\cdot)| \leq 0.1 g_2(\cdot) \end{cases} \quad (68)$$

These uncertainties can be seen as modelling errors or system disturbances [5]. The subsystem matrices are given by, $\forall i \in \Omega_4$

$$\begin{aligned} F_{x,i}^1 &= F_{x,i}^2 = \begin{bmatrix} 1 & 1 \\ 0 & 0 \end{bmatrix}; & B_{w,i}^1 &= B_{w,i}^2 = \begin{bmatrix} 0.1 \\ 0 \end{bmatrix}; \\ C_i^1 &= C_i^2 = [1 \quad 0]; & D_i^1 &= D_i^2 = 0.01 \end{aligned} \quad (69)$$

- *Region 1:* $\Pi \leq \varepsilon$ (low load region) (see (70))
- *Region 2:* $\Pi > \varepsilon$ (high load region) (see (71))

In this work, only system state constraints $P_{man,min} \leq P_{man} \leq P_{man,max}$ will be considered in control design. Hence, the polyhedral region P_x defined in (9) is with $h_m^T = [h_{P_{man,m}}, h_{x_{int,m}}] = [h_{P_{man,m}}, 0]$, $m = 1, 2$. Theorem 1 can be now applied to control the considered automotive application.

Remark 5: In T-S tracking control framework, it has been proved in [28] that the input-to-state stability propriety [29] according to the exogenous input y_{ref} is guaranteed since all normalised membership and indicator functions are bounded by construction.

Remark 6: Note also that all data concerning the turbocharged air system and controller will not be revealed here for the confidentiality reason with our industrial collaboration partners. However, this does not restrict our

$$\begin{cases} \text{Zone 1 : } \eta_1^1 = \omega_{11}^1 \cdot \omega_{12}^1; & \eta_2^1 = \omega_{11}^1 \cdot \omega_{22}^1; & \eta_3^1 = \omega_{21}^1 \cdot \omega_{12}^1; & \eta_4^1 = \omega_{21}^1 \cdot \omega_{22}^1 \\ \text{Zone 2 : } \eta_1^2 = \omega_{11}^2 \cdot \omega_{12}^2; & \eta_2^2 = \omega_{11}^2 \cdot \omega_{22}^2; & \eta_3^2 = \omega_{21}^2 \cdot \omega_{12}^2; & \eta_4^2 = \omega_{21}^2 \cdot \omega_{22}^2 \end{cases} \quad (63)$$

$$\begin{cases} \dot{\bar{x}} = \sum_{k=1}^2 \sum_{i=1}^4 \mu_k(P_{man}) \eta_i^k(\theta) \{ (\bar{A}_i^k + \Delta \bar{A}_i^k) \bar{x} + \bar{B}_{w,i}^k \tilde{w} + (\bar{B}_{u,i}^k + \Delta \bar{B}_{u,i}^k) \text{sat}(u) + B y_{ref} \} \\ y = \sum_{k=1}^2 \sum_{i=1}^4 \mu_k(P_{man}) \eta_i^k(\theta) (\bar{C}_i^k \bar{x} + \bar{D}_i^k w) \end{cases} \quad (66)$$

$$\begin{aligned} A_1^1 &= A_2^1 = \begin{bmatrix} -\bar{f}_1 & 0 \\ -1 & 0 \end{bmatrix}; & B_{u,1}^1 &= B_{u,3}^1 = \begin{bmatrix} \bar{f}_2 & 0 \\ 0 & 0 \end{bmatrix}; & E_{A,i}^1 &= \begin{bmatrix} -1.4 & 0 \\ 0 & 0 \end{bmatrix} \\ A_3^1 &= A_4^1 = \begin{bmatrix} -f_1 & 0 \\ -1 & 0 \end{bmatrix}; & B_{u,2}^1 &= B_{u,4}^1 = \begin{bmatrix} f_2 & 0 \\ 0 & 0 \end{bmatrix}; & E_{u,i}^1 &= \begin{bmatrix} 0 & 0 \\ 3513 & 0 \end{bmatrix} \end{aligned} \quad (70)$$

$$\begin{aligned} A_1^2 &= A_2^2 = \begin{bmatrix} \bar{g}_1 & 0 \\ -1 & 0 \end{bmatrix}; & B_{u,1}^2 &= B_{u,3}^2 = \begin{bmatrix} 0 & -\bar{g}_2 \\ 0 & 0 \end{bmatrix}; & E_{A,i}^2 &= \begin{bmatrix} 0.075 & 0 \\ 0 & 0 \end{bmatrix} \\ A_3^2 &= A_4^2 = \begin{bmatrix} g_1 & 0 \\ -1 & 0 \end{bmatrix}; & B_{u,2}^2 &= B_{u,4}^2 = \begin{bmatrix} 0 & -g_2 \\ 0 & 0 \end{bmatrix}; & E_{u,i}^2 &= \begin{bmatrix} 0 & 0 \\ 0 & -164 \end{bmatrix} \end{aligned} \quad (71)$$

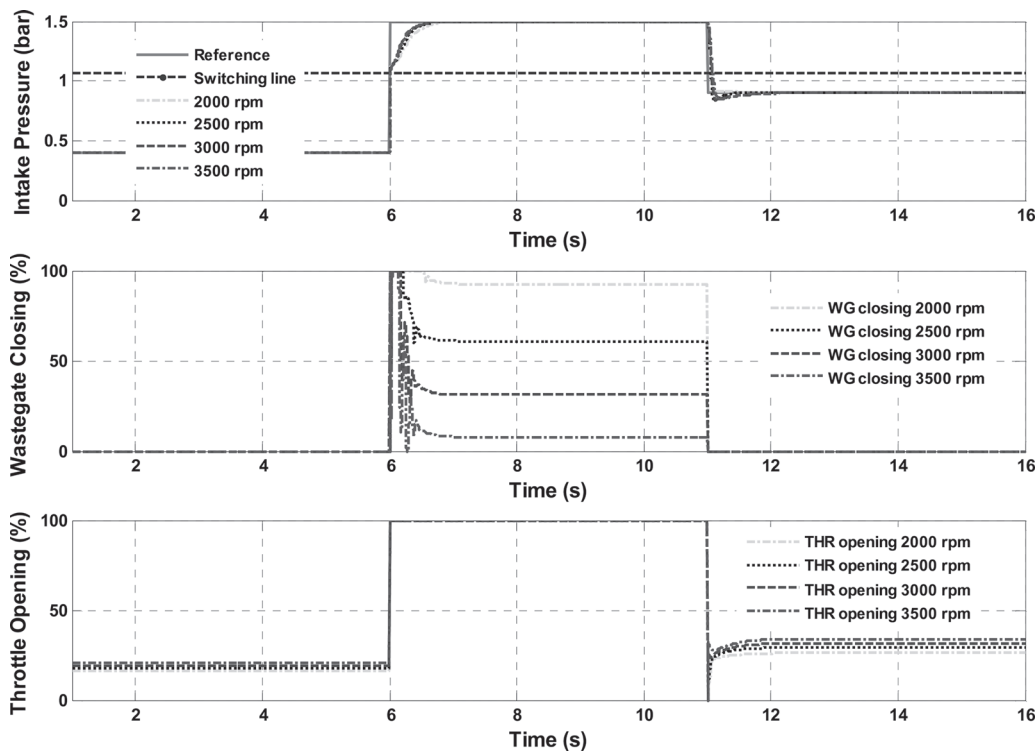


Fig. 5 Trajectory tracking with different engine speeds

observations since we are focusing on the control design and the controller performance.

Remark 7: As highlighted in [7], a typical phenomenon when dealing with switching control is non-continuity of control input at switching boundaries. It may lead to a serious degradation of the controller performance. To handle this problem, the ‘distance’ between all the connecting gains in all the regions should be minimised as much as possible [7]. Concretely, the smoothness condition $L_2^1 \simeq L_1^2$ will be integrated together with LMI conditions in Theorem 1 to design the feedback gains. From (36), the smoothness LMI condition is fulfilled if

$$\begin{bmatrix} \beta I & * \\ (Y_2^1 - Y_1^2) & I \end{bmatrix} \geq 0 \quad (72)$$

where $\beta > 0$ should be minimised.

Remark 8: The controller feedback gains L_j^k and K_j^k , $\forall (k, j) \in \Omega_2 \times \Omega_4$ in (65) are now efficiently designed by solving the LMI conditions in Theorem 1 and also the smoothness condition (72) with some available numerical tools [14].

4.4 Simulation results and analysis

Hereafter, a series of trials will be performed to point out the validity of the proposed method. For the sake of clarity, the two commands (throttle, wastegate) are normalised. The control inputs constraints in (53) become: $0 \leq \bar{u}_{thr}, \bar{u}_{wg} \leq 100\%$. When $\bar{u}_{thr} = 100\%$ (resp. $\bar{u}_{wg} = 0\%$), it means that the throttle (resp. wastegate) is fully open. On the reverse, when $\bar{u}_{thr} = 0\%$ (resp. $\bar{u}_{wg} = 100\%$), the throttle (resp. wastegate) is fully closed. Before starting, note that the proposed controller is easily tuned with only two parameters, the decay rate α and the disturbance attenuation level γ which are the same for all simulations.

4.4.1 Test 1: control strategy validation: This scenario test aims at validating turbocharged air system control strategy stated above and showing the pressure trajectory tracking performance at different engine speeds. To this end, the intake pressure reference varies in different engine operating regions for different engine speeds (from 2000 up to 3500 rpm). The validity of the proposed control strategy is confirmed by the results in Fig. 5. Several remarks on these results can be reported as follows. Firstly, the convergence is ensured over the whole considered operating range. The wastegate response is very aggressive during the turbocharger transients; it hits the constraints and then stabilises to track the boost pressure. This behaviour which can be tuned easily with the decay rate α allows compensating the slow dynamics of the turbocharger. Secondly, the wastegate is open in low load operating region. Once the throttle is fully open, the wastegate closes to track the boost pressure which is approximately equal to the intake pressure in this case. This switching strategy allows minimising the engine pumping losses [4, 17]. Finally, the controller does not generate any overshoot in the considered operating range which is also a very-important property for the driving comfort.

Remark 9: In low load region (Region 1), the wastegate is fully open, that is, $\bar{u}_{wg} = 100\%$. Note that this imposed constant value does not agree with the one computed from the feedback gains L_j^1 and K_j^1 , $\forall j \in \Omega_4$. However, fortunately, it can be observed from the matrices $B_{u,i}^1$, $\forall i \in \Omega_4$ that this constant control input will never act on the dynamics of the closed-loop system in this region. The same remark can be done for high load region (Region 2) with $\bar{u}_{thr} = 100\%$.

4.4.2 Test 3: vehicle transients: The closed-loop responses during the vehicle transient are presented in Fig. 6. It can be noted that the proposed controller is perfectly able to guarantee a very-good tracking performance even with the

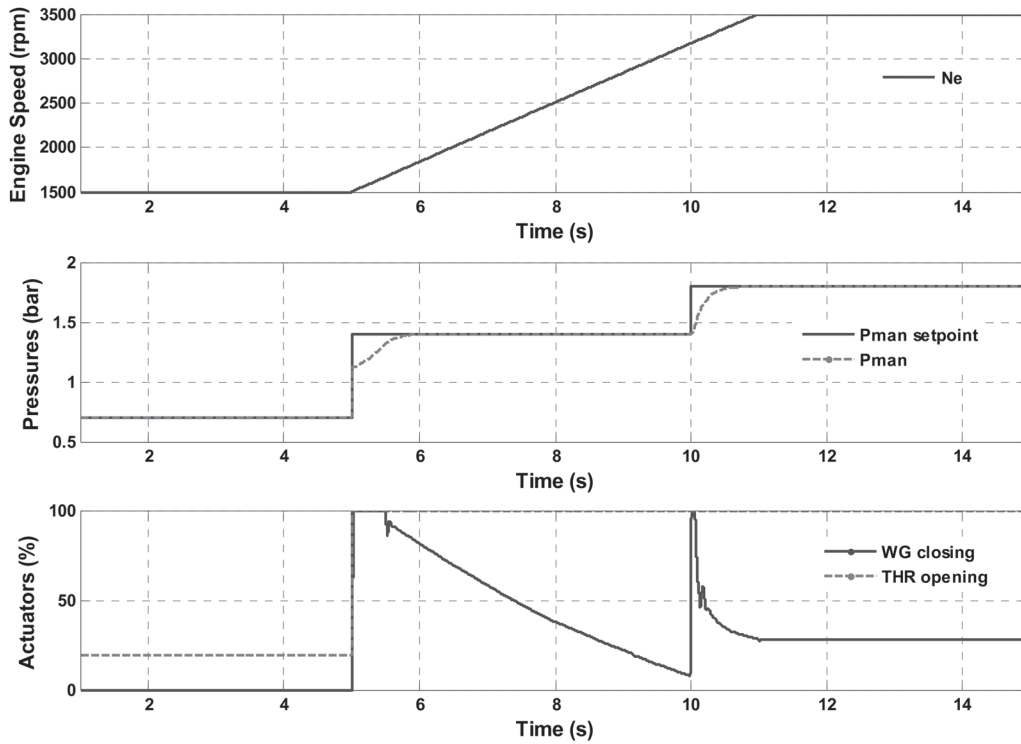


Fig. 6 Variation of engine speed (up) and pressure tracking performance (middle) with corresponding actuator commands (bottom) for a vehicle transient

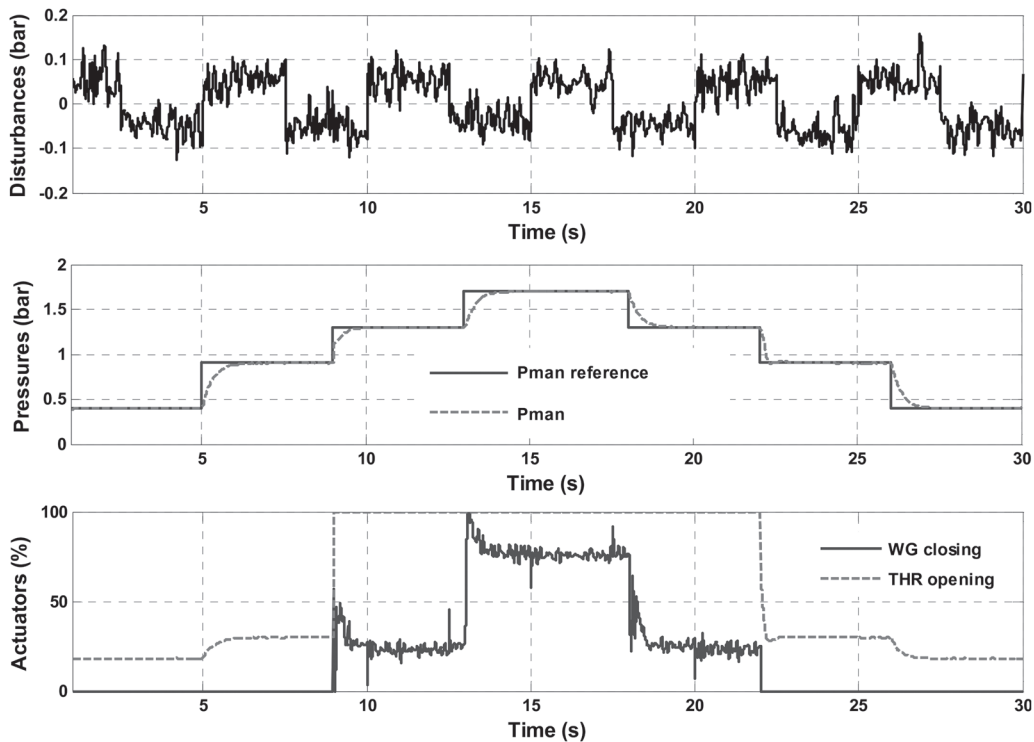


Fig. 7 Disturbance used for the simulation (top); Intake pressure trajectory tracking (middle); and actuators corresponding solicitation (bottom) at $N_e = 2750$ rpm

important variation of the engine speed (which represents the vehicle transient).

4.4.3 Test 4: disturbance attenuation: This test aims at showing the robustness performance (w.r.t the exogenous disturbances) and the benefits of the integral action in the

control loop. For that, the intake pressure reference varies largely at constant speed, and a special bounded noise w , which is the combination of a sampled Gaussian noise with a square wave, is also added (see Fig. 7 – top). Despite the presence of noise as shown in Fig. 7 (middle), the tracking is still guaranteed without any offset in steady-state phases and the disturbance is also well attenuated. However, the

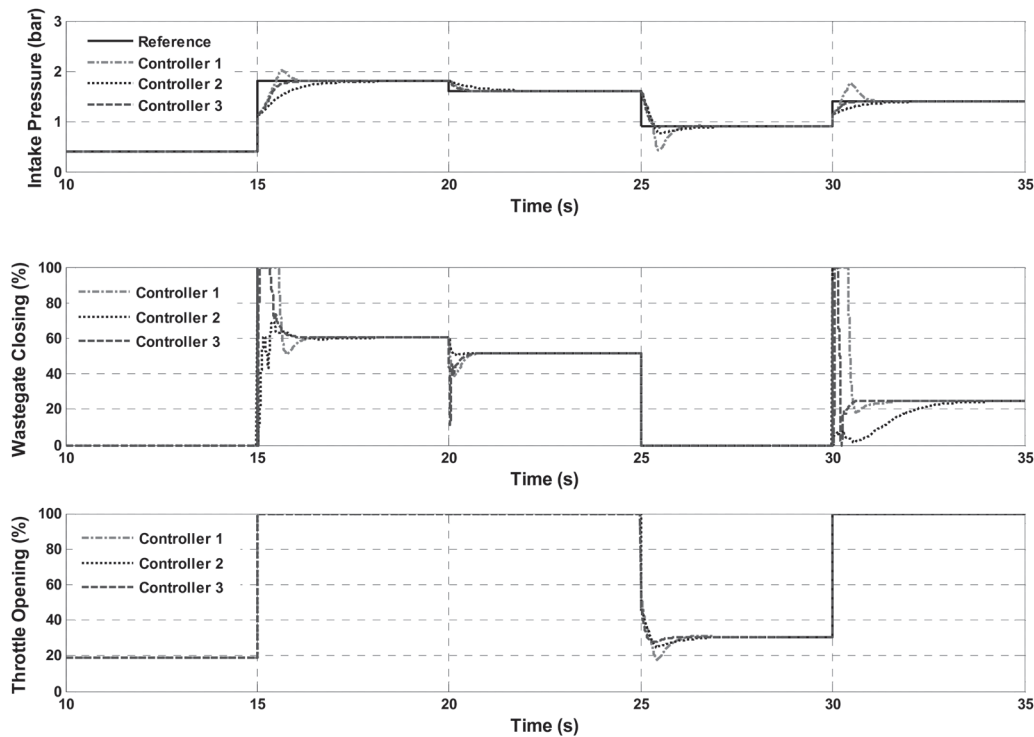


Fig. 8 Closed-loop performance comparison with different control approaches

wastegate solicitation is sensitive to noises Fig. 7 (bottom). It is because of the non-minimum phase zero in the relation between the wastegate behaviour and the boost pressure [5, 30].

4.4.4 Test 5: with and without saturation: Control input saturation is a major control issue of industrial systems. It must be taken into account in the control design to guarantee the closed-loop stability and improve the control performance. This fact will be pointed out in this part. Our proposed method will be also compared to the existing results in [7].

Fig. 8 shows the system responses with different control approaches: Controller 1 does not take into account the actuator saturation in the control design, Controller 2 is with the unsaturated control approach proposed in [7] and Controller 3 is with our proposed method. Note that the initial states are taken as $\bar{x}(0) \triangleq [P_{\text{man}}(0); x_{\text{int}}(0)] = [0.5; 0]$ to design Controller 2 and its decay rate is also decreased in comparison with the one of Controller 3 to obtain the feasibility solution. Some observations on the results in Fig. 8 can be remarked. Firstly, Controller 1 takes much more time to stabilise the system and it leads to important pressure overshoots which must be absolutely avoided to ensure an acceptable driving comfort. Secondly, actuator responses of the Controller 2 are over-constrained; control performance is therefore rather poor in terms of time response. Finally, Controller 3 achieves a very-satisfying performance (no overshoots, quick time response) and fulfils our control specifications.

5 Conclusions

The purpose of this work was to develop a new approach to design robust controllers for switching uncertain T-S systems subject to both control input and state constraints.

Based on Lyapunov stability theory, a constructive control design procedure is provided. In this paper, the control input saturation is dealt with by using a polytopic representation. The feedback gains can be efficiently computed with some numerical tools since the control design is formulated as an LMI optimisation problem. It has been proved that, compared to existing results, the proposed approach provides less conservative design conditions and the guaranteed domain of attraction is maximised. At the end, the control of a turbocharged air system of an SI engine was considered to illustrate the effectiveness of the proposed method in industrial context.

6 Acknowledgments

This research is sponsored by the International Campus on Safety and Intermodality in Transportation the Nord-Pas-de-Calais Region, the European Community, the Regional Delegation for Research and Technology, and the French National Center for Scientific Research. This work is also sponsored by VALEO Company through the SURAL'HY project.

7 References

- 1 Takagi, T., Sugeno, M.: 'Fuzzy identification of systems and its applications to modeling and control', *IEEE Trans. Syst. Man Cybern.*, 1985, **15**, (1), pp. 116–132
- 2 Tanaka, K., Wang, H.O.: 'Fuzzy control systems design and analysis: a linear matrix inequality approach' (Wiley, Wiley-Interscience, New York, 2001)
- 3 Feng, G.: 'A survey on analysis and design of model-based fuzzy control systems', *IEEE Trans. Fuzzy Syst.*, 2006, **14**, (5), pp. 676–697
- 4 Nguyen, A.T., Lauber, J., Dambrine, M.: 'Switching fuzzy control of the air system of a turbocharged SI engine'. *IEEE Int. Conf. on Fuzzy Systems*, Brisbane, Australia, 2012, pp. 893–899
- 5 Nguyen, A.T., Lauber, J., Dambrine, M.: 'Robust H_∞ control design for switching uncertain system: application for turbocharged gasoline

- air system control'. 51st Conf. on Decision and Control, Maui, Hawaii, USA, 2012, pp. 4265–4270
- 6 Mamdani, E.H.: 'Application of fuzzy algorithms for control of simple dynamic plant', *Proc. Inst. Electr. Engineers*, 1974, **121**, (12), pp. 1585–1588
 - 7 Tanaka, K., Iwasaki, M., Wang, H.O.: 'Switching control of an R/C hovercraft: stabilization and smooth switching', *IEEE Trans. Syst. Man Cybern.*, 2001, **31**, (6), pp. 853–863
 - 8 Taniguchi, T., Tanaka, K., Ohtake, H., Wang, H.O.: 'Model construction, rule reduction, and robust compensation for generalized form of Takagi–Sugeno fuzzy systems', *IEEE Trans. Fuzzy Syst.*, 2001, **9**, (4), pp. 525–538
 - 9 Liberzon, D.: 'Switching in systems and control' (Birkhauser, Boston, MA, 2003)
 - 10 Cao, Y.Y., Lin, Z.: 'Robust stability analysis and fuzzy-scheduling control for nonlinear systems subject to actuator saturation', *IEEE Trans. Fuzzy Syst.*, 2003, **11**, (1), pp. 57–67
 - 11 Fang, H., Lin, Z., Hu, T.: 'Analysis of linear systems in the presence of actuator saturation and \mathcal{L}_2 disturbances', *Automatica*, 2004, **40**, pp. 1229–1238
 - 12 Tarbouriech, S., Garcia, G., Gomes, da Silva, J.M. Jr., Queinnec I.: 'Stability and stabilization of linear systems with saturating actuators' (Springer-Verlag, London, 2011)
 - 13 Kothare, M.V., Campo, P.J., Morari, M., Nett, C.N.: 'A unified framework for the study of anti-windup designs', *Automatica*, 1994, **30**, (12), pp. 1869–1883
 - 14 Gahinet, P., Nemirovski, A., Laub, A.J., Chilali, M.: 'LMI control toolbox' (The Math Works Inc, 1995)
 - 15 Lee, K.R., Jeung, E.T., Park, H.B.: 'Robust fuzzy H_∞ control for uncertain nonlinear systems via state feedback: an LMI approach', *Fuzzy Sets Syst.*, 2001, **120**, (1), pp. 123–134
 - 16 Yoneyama, J.: 'Robust H_∞ control analysis and synthesis for takagi–sugeno general uncertain fuzzy systems', *Fuzzy Sets Syst.*, 2006, **157**, (16), pp. 2205–2223
 - 17 Eriksson, L., Frei, S., Onder, C., Guzzella, L.: 'Control and optimization of turbocharged SI engines'. 15th IFAC World Congress, Barcelona, Spain, 2002
 - 18 Nguyen, A.T., Lauber, J., Dambrine, M.: 'Modeling and switching fuzzy control of the air path of a turbocharged spark ignition engine'. IFAC Workshop on Engine and Powertrain Control, Simulation and Modeling, Paris, France, 2012, pp. 138–145
 - 19 Boyd, S., Ghaoui, L.E., Feron, E., Balakrishnan, V.: 'Linear matrix inequalities in system and control theory' (Society for Industrial and Applied Mathematics (SIAM), Philadelphia, 1994)
 - 20 Petersen, I.R.: 'A stabilization algorithm for a class of uncertain linear systems', *Syst. Control Lett.*, 1987, **8**, (4), pp. 351–357
 - 21 Tuan, H., Apkarian, P., Narikiyo, T., Yamamoto, Y.: 'Parameterized linear matrix inequality techniques in fuzzy control system design', *IEEE Trans. Fuzzy Syst.*, 2001, **9**, (2), pp. 324–332
 - 22 Liu, X., Zhang, Q.: 'New approaches to controller designs based on fuzzy observers for T–S fuzzy systems via LMI', *Automatica*, 2003, **39**, (9), pp. 1571–1582
 - 23 Sala, A., Arino, C.: 'Asymptotically necessary and sufficient conditions for stability and performance in fuzzy control: applications of Polya's theorem', *Fuzzy Sets Syst.*, 2007, **158**, pp. 2671–2686
 - 24 Castelan, E.B., Tarbouriech, S., Gomes, da Silva, J.M. Jr., Queinnec, I.: ' \mathcal{L}_2 -stabilization of continuous-time linear systems with saturating actuators', *Int. J. Robust Nonlinear Control*, 2006, **16**, pp. 935–944
 - 25 Guzzella, L., Onder, C.: 'Introduction to modeling and control of internal combustion engine systems' (Springer, 2004)
 - 26 Khier, D., Lauber, J., Floquet, T., *et al.*: 'Robust Takagi–Sugeno fuzzy control of a spark ignition engine', *Control Eng. Pract.*, 2007, **15**, pp. 1446–1456
 - 27 Moulin, P., Chauvin, J.: 'Modeling and control of the air system of a turbocharged gasoline engine', *Control Eng. Pract.*, 2011, **19**, (3), pp. 287–297
 - 28 Lendek, Zs., Guerra, T.M., Babuška R., De Schutter B.: 'Stability analysis and nonlinear observer design using Takagi–Sugeno fuzzy models', 'Studies in Fuzziness and Soft Computing' (Springer, 2010)
 - 29 Sontag, E.D., Wang, Y.: 'On characterizations of the input to state stability property', *Syst. Control Lett.*, 1995, **24**, (5), pp. 351–359
 - 30 Karnik, A., Buckland, J., Freudenberg, J.: 'Electronic throttle and wastegate control for turbocharged gasoline engines'. American Control Conf., Portland, 2005, pp. 4434–4439